

THE MATHEMATICS OF TAFFY PULLERS

JEAN-LUC THIFFEAULT

ABSTRACT. We describe a number of devices for pulling candy, called taffy pullers, that are related to pseudo-Anosov maps of punctured spheres. Though the mathematical connection has long been known for the two most common taffy puller models, we unearth a rich variety of early designs from the patent literature, and introduce a new one.

INTRODUCTION

Taffy is a type of candy made by first heating sugar to a critical temperature, letting the mixture cool on a slab, then repeatedly ‘pulling’ — stretching and folding — the resulting mass. The purpose of pulling is to get air bubbles into the taffy, which gives it a nicer texture. Many devices have been built to assist pulling, and they all consist of a collection of fixed and moving rods, or pins. Figure 1 shows the action of such a taffy puller from an old patent. Observe that the taffy (pictured as a dark mass) is stretched and folded on itself repeatedly. As the rods move, the taffy is caught on the rods and its length is forced to grow exponentially. The effectiveness of a taffy puller is directly proportional to this growth, since more growth implies a more rapid trapping of the air bubbles. Given a pattern of periodic rod motion, regarded as orbits of points in the plane, the mathematical challenge is to compute the growth.

We will describe in broad terms how the computation of growth is achieved. The framework involves the topological dynamics ideas pioneered by William Thurston, but we will shy away from a complete treatment involving rigorous definitions. Instead we will boil down the computation to its essence: the relationship between maps of the torus and those on a punctured sphere. Computations on the former involve simple linear algebra, and the taffy pullers are described by the latter. We will also show an explicit example that involves surfaces of higher genus than a torus, which allow us to describe taffy pullers with more than three or four moving rods. Throughout, we will give examples of taffy pullers from the patent literature as well as a newly-invented one. Finally, we answer the question: which taffy puller is the ‘best’ in a mathematical sense?

Supported by NSF grant CMMI-1233935. Contains an extra appendix compared to the version published in *Mathematical Intelligencer*.

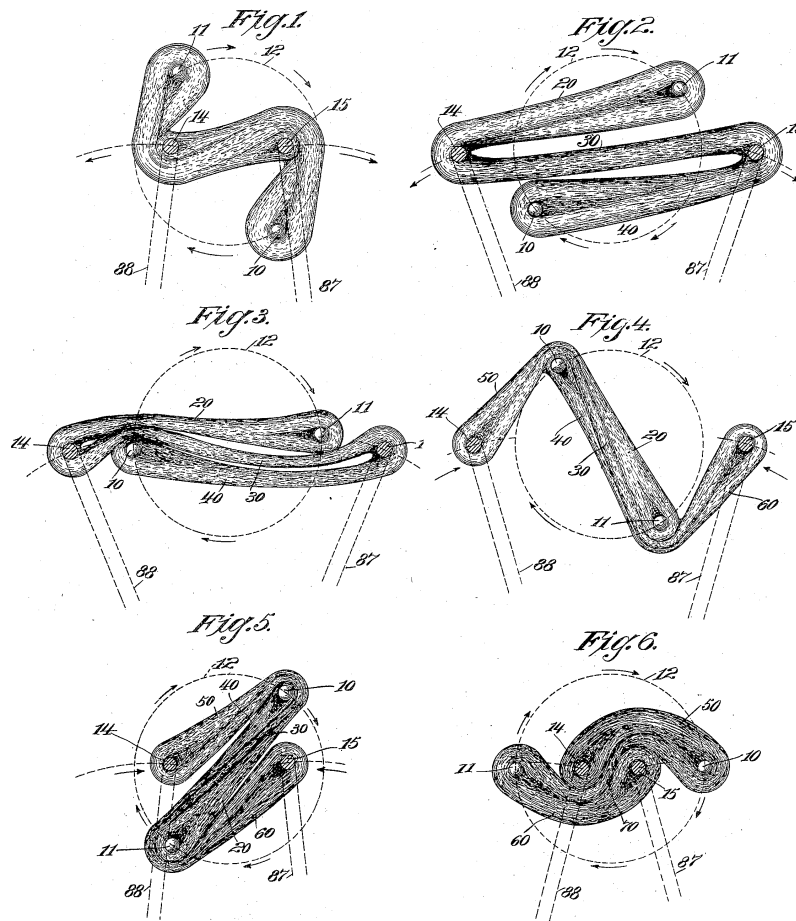


FIGURE 1. Action of the taffy puller patented by Richards (1905). The rod motion is equivalent (conjugate) to that of Fig. 6.

SOME HISTORY

Until the late 19th century, taffy was pulled by hand — an arduous task. The process was ripe for mechanization. The first patent for a mechanical taffy puller was by Firchau (1893): his design consisted of two counter-rotating rods on concentric circles. This is not a ‘true’ taffy puller: a piece of taffy wrapped around the rods will not grow exponentially. Firchau’s device would have been terrible at pulling taffy, but it was likely never built.

In 1900, Herbert M. Dickinson invented the first nontrivial taffy puller, and described it in the trade journal *The Confectioner*. His machine involved a fixed rod and two rods that move back-and-forth. The moving rods are ‘tripped’ to

exchange position when they reach the limit of their motion. Dickinson later patented the machine (Dickinson 1906) and assigned it to Herbert L. Hildreth, the owner of the Hotel Velvet on Old Orchard Beach, Maine. Taffy was especially popular at beach resorts, in the form of salt water taffy (which is not really made using salt water). Hildreth sold his 'Hildreth's Original and Only Velvet Candy' to the Maine tourists as well as wholesale, so he needed to make large quantities of taffy. Though he was usually not the inventor, he was the assignee on several taffy puller patents in the early 1900s. In fact several such patents were filed in a span of a few years by several inventors, which led to lengthy legal wranglings. Some of these legal issues were resolved by Hildreth buying out the other inventors; for instance, he acquired one patent for \$75,000 (about two million of today's dollars). Taffy was becoming big business.

Shockingly, the taffy patent wars went all the way to the US Supreme Court. The opinion of the Court was delivered by Chief Justice William Howard Taft. The opinion shows a keen grasp of topological dynamics (*Hildreth v. Mastoras*, 1921):

The machine shown in the Firchau patent [has two pins that] pass each other twice during each revolution [. . .] and move in concentric circles, but do not have the relative in-and-out motion or Figure 8 movement of the Dickinson machine. With only two hooks there could be no lapping of the candy, because there was no third pin to re-engage the candy while it was held between the other two pins. The movement of the two pins in concentric circles might stretch it somewhat and stir it, but it would not pull it in the sense of the art.

The Supreme Court opinion displays the fundamental insight that at least three rods are required to produce some sort of rapid growth. Moreover, the 'Figure 8' motion is identified as key to this growth. We shall have more to say on this rod motion as we examine in turn the different design principles.

The Dickinson taffy puller may have been the first, but it was overly complicated and likely never used to make large quantities of candy. A similar rod motion can be obtained by a much simpler mechanism, which was introduced in a patent by Robinson and Deiter (1908) and is still in use today. In this device, two rods move in counter-rotating orbits around a fixed rod (Fig. 2). We call this design the *standard 3-rod taffy puller*.

THREE-ROD TAFFY PULLERS

Taffy pullers involving three rods (some of which may be fixed) are the easiest to describe mathematically. The action of arguably the simplest such puller, from the mathematical standpoint, is depicted in Fig. 3(a). By action, we mean the effect of the puller on a piece of abstract 'taffy.' For this puller, the first and second rods are

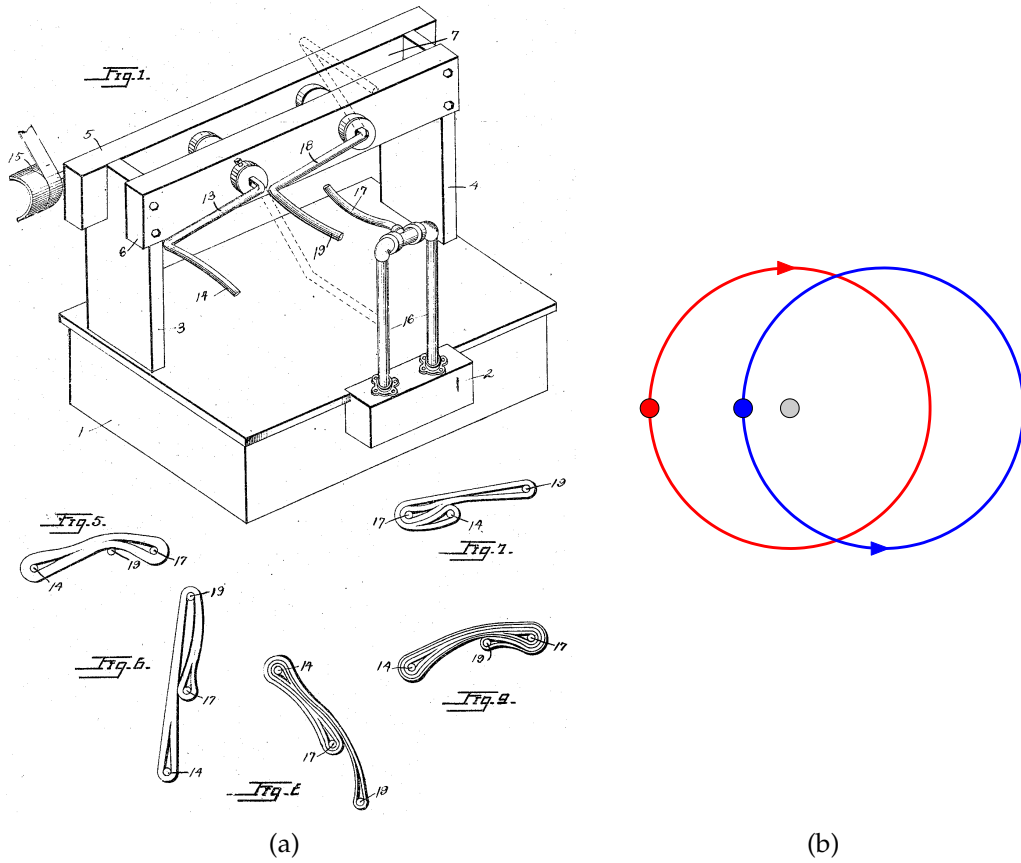


FIGURE 2. (a) Taffy puller from the patent of Robinson and Deiter (1908). (b) The motion of the rods.

interchanged clockwise, then the second and third are interchanged counterclockwise. Notice that each rod undergoes a ‘Figure 8’ motion, as shown in Fig. 3(b) for $\frac{1}{3}$ period.

We now demonstrate that such a taffy puller motion arises naturally from linear maps on the torus. (We leave out many mathematical details — see for example Farb and Margalit (2011), Fathi, Laudenbach, and Poénaru (1979), and Thurston (1988) for the full story.) We use the standard model of the torus T^2 as the unit square $[0, 1]^2$ with opposite edges identified. Consider the linear map $\iota : T^2 \rightarrow T^2$, defined by $\iota(x) = -x \pmod 1$. The map ι is an involution ($\iota^2 = \text{id}$) with four fixed points on the torus $[0, 1]^2$,

$$(1) \quad p_0 = (0 \ 0), \quad p_1 = \left(\frac{1}{2} \ 0\right), \quad p_2 = \left(\frac{1}{2} \ \frac{1}{2}\right), \quad p_3 = \left(0 \ \frac{1}{2}\right).$$

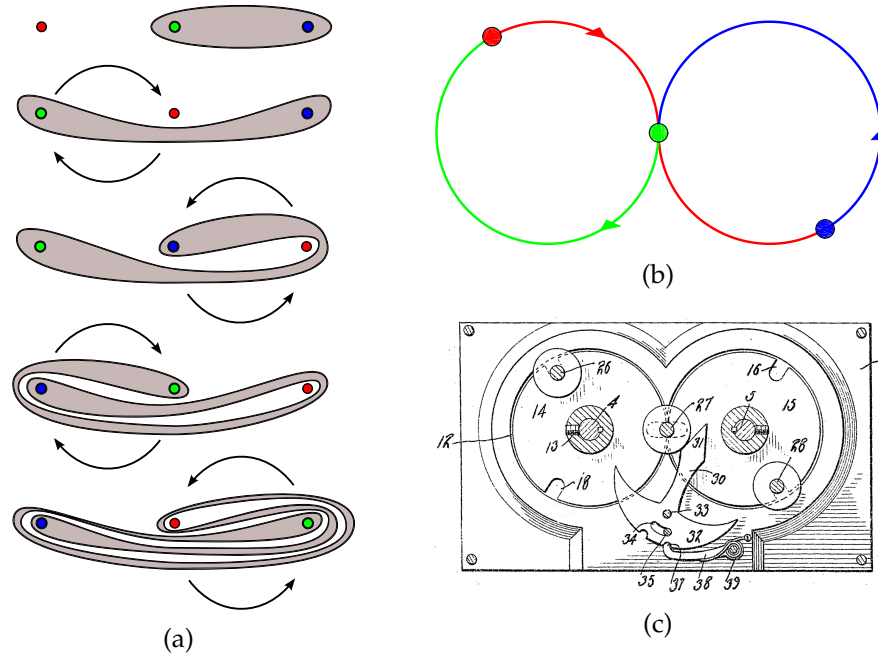


FIGURE 3. (a) The action of a 3-rod taffy puller. The first and second rods are interchanged clockwise, then the second and third rods are interchanged counterclockwise. (b) Each of the three rods moves in a Figure-8. (c) Taffy puller from the patent of Nitz (1918), where rods alternate between the two wheels.

Figure 4(a) shows how the different sections of T^2 are mapped to each other under ι ; arrows map to each other or are identified because of periodicity. The quotient space $S = T^2/\iota$, depicted in Fig. 4(b), is actually a sphere in the topological sense (it has genus zero). We can see this by ‘gluing’ the identified edges to obtain Fig. 4(c). The 4 fixed points of ι above will play a special role, so we puncture the sphere at those points and write $S = S_{0,4}$, which indicates a surface of genus 0 with 4 punctures.

Now let’s take a general linear map $\phi : T^2 \rightarrow T^2$. We write $\phi(x) = M \cdot x \pmod 1$, with $x \in [0, 1]^2$ and M a matrix in $SL_2(\mathbb{Z})$,

$$(2) \quad M = \begin{pmatrix} a & b \\ c & d \end{pmatrix}, \quad a, b, c, d \in \mathbb{Z}, \quad ad - bc = 1.$$

This guarantees that ϕ is an orientation-preserving homeomorphism — a continuous map of T^2 with a continuous inverse. The map ϕ fixes $p_0 = (0 \ 0)$ and *permutes*

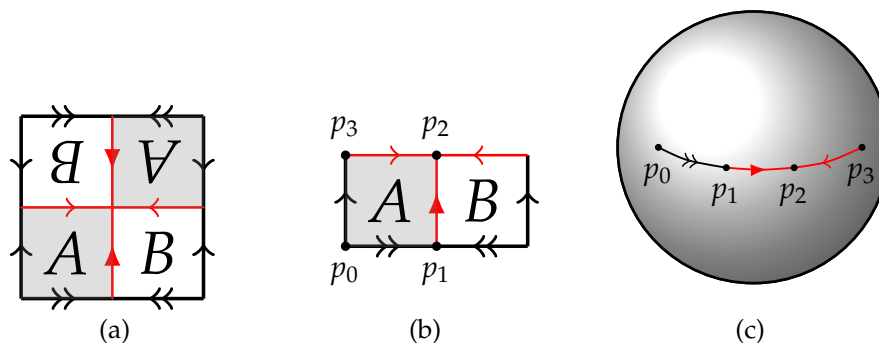


FIGURE 4. (a) Identification of regions on $T^2 = [0, 1]^2$ under the map ι . (b) The surface $S = T^2/\iota$, with the four fixed points of ι shown. (c) S is a sphere with four punctures, denoted $S_{0,4}$.

the ordered set (p_1, p_2, p_3) . For example, the map

$$(3) \quad \phi(x) = \begin{pmatrix} 2 & 1 \\ 1 & 1 \end{pmatrix} \cdot x \pmod 1$$

maps (p_1, p_2, p_3) to (p_3, p_1, p_2) . This is an *Anosov map*: it has a real eigenvalue larger than one (in magnitude). We call the spectral radius λ of the matrix M the *dilatation* of the map ϕ . A key fact is that the length of any noncontractible simple closed curve on T^2 grows as λ^n as the number of iterates $n \rightarrow \infty$ (Fathi, Laudenbach, and Poénaru 1979).

Because $\iota \circ \phi = \phi \circ \iota$, a linear map such as ϕ on the torus projects nicely to the punctured sphere $S_{0,4} = T^2/\iota$. The induced map on $S_{0,4}$ is called *pseudo-Anosov* rather than Anosov, since the quotient of the torus by ι created four singularities. (We shall not need precise definitions of these terms; here by Anosov map we mean a linear map on the torus with spectral radius larger than 1, and by pseudo-Anosov we mean the same map projected to $S_{0,4}$.)

Let's see how the action of the map (3) gives the taffy puller in Fig. 3. The permuted points (p_1, p_2, p_3) play the role of the rods of the taffy puller. Figure 5(a) (left) shows two curves on the torus, which project to curves on the punctured sphere $S_{0,4}$ (right). (Whenever we say curve, we will actually mean an equivalence class of curves under homotopy fixing the punctures.) The blue curve from p_2 to p_3 should be identified with the piece of taffy in Fig. 3(a). Now if we act on the curves with the torus map (3), we obtain the curves in Fig. 5(b) (left). After taking the quotient with ι , the curves project down as in Fig. 5(b) (right). This has the same shape as our taffy in Fig. 3(a) (third frame) for $\frac{1}{3}$ period of the taffy puller.

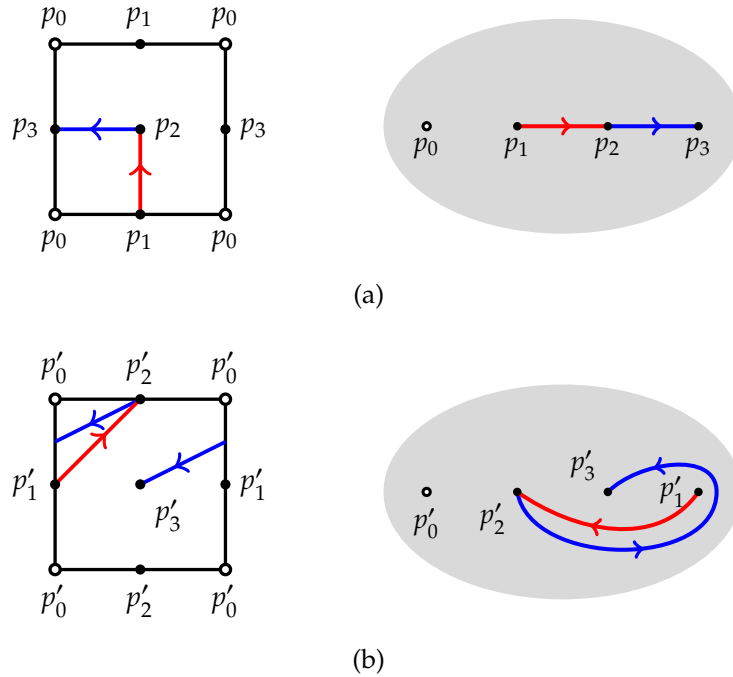


FIGURE 5. (a) Two curves on the torus T^2 (left), which project to curves on the punctured sphere $S_{0,4}$ (right). (b) The two curves transformed by the map (3) (left), and projected onto $S_{0,4}$ (right). The transformed blue curve is the same as in the third frame of Fig. 3(a).

What we've essentially shown is that the taffy puller in Fig. 3 can be described by projecting the Anosov map (3) of the torus to a pseudo-Anosov map of $S_{0,4}$. The growth of the length of taffy, under repeated action, will be given by the spectral radius λ of the matrix M , here $\lambda = \varphi^2$ with φ being the Golden Ratio $\frac{1}{2}(1 + \sqrt{5})$. This taffy puller is a bit peculiar in that it requires rods to move in a Figure-8 motion, as shown in Fig. 3(b). This is challenging to achieve mechanically, but surprisingly such a device was patented by Nitz (1918) (Fig. 3(c)), and then apparently again by Kirsch (1928). The device requires rods to alternately jump between two rotating wheels.

All 3-rod devices can be treated in the same manner, including the standard 3-rod taffy puller depicted in Fig. 2. We will not give the details here, but it can be shown to arise from the linear map

$$(4) \quad \phi(x) = \begin{pmatrix} 5 & 2 \\ 2 & 1 \end{pmatrix} \cdot x \pmod{1}$$

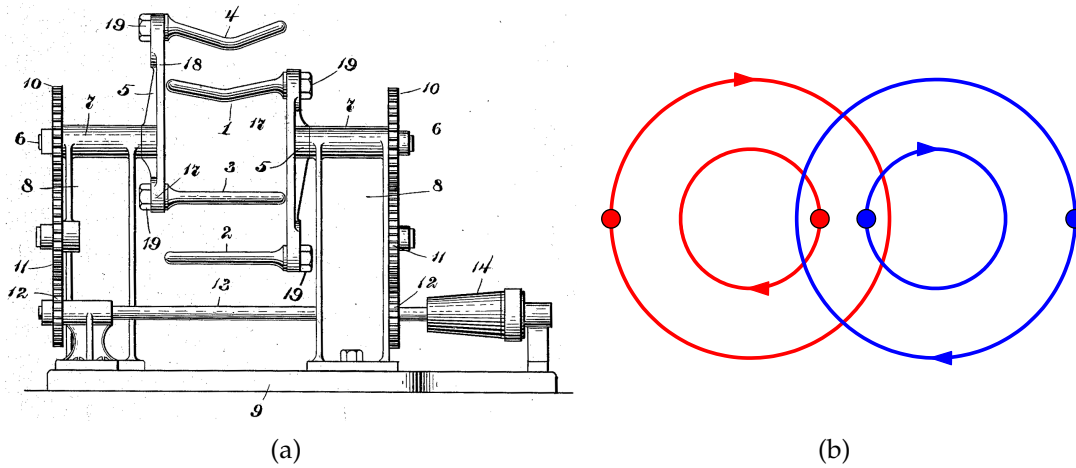


FIGURE 6. (a) Side view of the standard 4-rod taffy puller from the patent of Thibodeau (1903), with four rotating rods set on two axes. (b) Rod motion.

which has $\lambda = \chi^2$. Here $\chi = 1 + \sqrt{2}$ is the *Silver Ratio* (Finn and Thiffeault 2011).

ARE FOUR RODS BETTER THAN THREE?

As discussed in the previous section, all 3-rod taffy pullers arise from Anosov maps of the torus. This is not true in general for more than three rods, but it is true for several specific devices. Probably the most common device is the *standard 4-rod taffy puller*, which was invented by Thibodeau (1903) and is shown in Fig. 6. It seems to have been rediscovered several times, such as by Hudson (1904). The design of Richards (1905) is a variation that achieves the same effect, and his patent has some of the prettiest diagrams of taffy pulling in action (Fig. 1). Mathematically, the 4-rod puller was studied by MacKay (2001) and Halbert and Yorke (2014).

The rod motion for the standard 4-rod puller is shown in Fig. 6(b). Observe that the two orbits of smaller radius are not intertwined, so topologically they might as well be fixed rods. This taffy puller arises from an Anosov map such as (4), but with all four points (p_0, p_1, p_2, p_3) of $S_{0,4}$ identified with rods. We relabel the four points (p_0, p_1, p_2, p_3) as $(1, 4, 3, 2)$, as in Fig. 7(a) (left), which gives the order of the rods on the right in that figure. The boundary point labeled 0 plays no direct

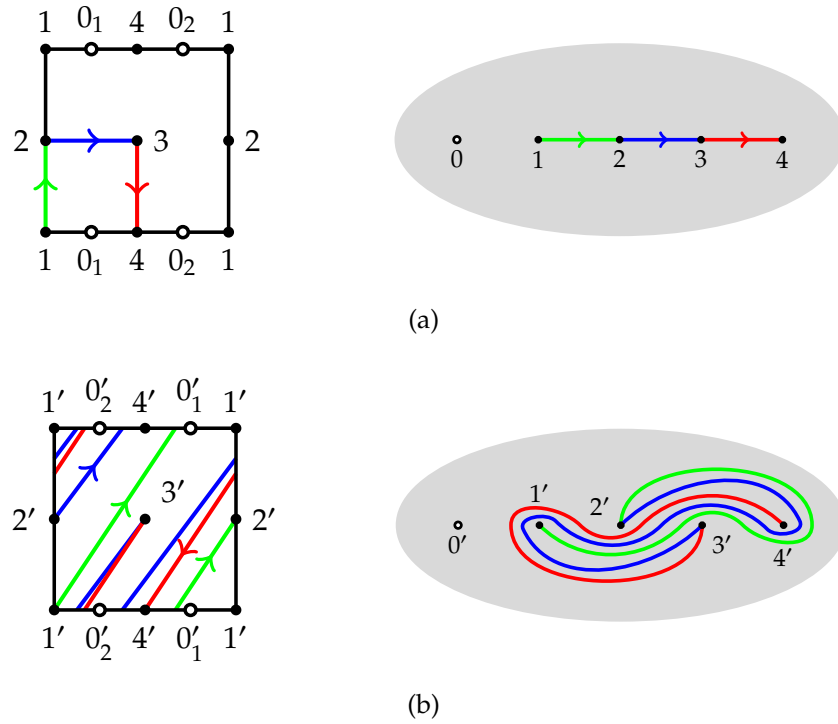


FIGURE 7. (a) Three curves on the torus T^2 (left), which project to curves on the punctured sphere $S_{0,5}$ (right). (b) The three curves transformed by the map (5) (left), and projected onto $S_{0,5}$ (right). Compare these to the last frame of Fig. 1.

role, but prevents us from shortening curves by passing them ‘behind’ the sphere.¹ Puncturing at this extra point gives the space $S_{0,5}$, the sphere with 5 punctures.

¹In the 3-rod case, the point labeled 0 in Fig. 5 plays this role. In the 4-rod case, we need to use $S_{0,5}$ in order to allow for this extra point. There are no more fixed points available, since $\phi(x)$ in (5) only has 4. However, a period-2 point of ϕ will do, as long as the two iterates are also mapped to each other by ι . The map (5) actually has 14 orbits of period 2, but only two of those are also invariant under ι :

$$\left\{ \left(\frac{1}{4} \ 0 \right), \left(\frac{3}{4} \ 0 \right) \right\} \quad \text{and} \quad \left\{ \left(\frac{1}{4} \ \frac{1}{2} \right), \left(\frac{3}{4} \ \frac{1}{2} \right) \right\}.$$

The second choice would put the boundary point being between two rods, so we choose the first orbit. The two iterates are labeled 0_1 and 0_2 in Fig. 7(a). They are interchanged in Fig. 7(b) after applying the map (5), but they both map to the same point on the sphere $S_{0,5} = (T^2/\iota) - \{0\}$, since they also satisfy $\iota(0_1) = 0_2$.

Now act on the curves in Fig. 7(a) with the map

$$(5) \quad \phi(x) = \begin{pmatrix} 3 & 2 \\ 4 & 3 \end{pmatrix} \cdot x \pmod{1}.$$

This map fixes each of the points 1, 2, 3, 4, just as the 4-rod taffy puller does. Figure 7(b) shows the action of the map on curves anchored on the rods: it acts in exactly the same manner as the standard 4-rod taffy puller. In fact,

$$(6) \quad \begin{pmatrix} 3 & 2 \\ 4 & 3 \end{pmatrix} = \begin{pmatrix} 1 & 0 \\ 1 & 1 \end{pmatrix} \begin{pmatrix} 5 & 2 \\ 2 & 1 \end{pmatrix} \begin{pmatrix} 1 & 0 \\ 1 & 1 \end{pmatrix}^{-1}$$

which means that the maps (4) and (5) are *conjugate* to each other. Conjugate maps have the same dilatation (the trace is invariant), so the standard 3-rod and 4-rod taffy pullers arise from essentially the same Anosov map, only interpreted differently. In other words, at least for the standard 4-rod puller, the addition of a rod does *not* increase the effectiveness of the device.

A NEW DEVICE

All the devices we described so far arise from maps of the torus. Now we give an example of a device that arises from a *branched cover* of the torus, rather than directly from the torus itself. (A theorem of Franks and Rykken (1999) implies that the dilatation λ must also be quadratic in this case.) Figure 8 shows such a device, designed and built by Alexander Flanagan and the author. It is a simple modification of the standard 4-rod design (Fig. 6), except that the two arms are of equal length, and the axles are extended to become fixed rods. There are thus 6 rods in play, and we shall see that this device has a rather large dilatation.

The construction of a map describing this 6-rod device uses the two involutions of the closed (unpunctured) genus two surface S_2 shown in Fig. 9. Imagine that an Anosov map gives the dynamics on the left ‘torus’ of the surface. The involution ι_1 extends those dynamics to a genus two surface. The involution ι_2 is then used to create the quotient surface $S_{0,6} = S_2/\iota_2$. The 6 punctures will correspond to the rods of the taffy puller.

A bit of experimentation suggests starting from the Anosov map

$$(7) \quad \phi(x) = \begin{pmatrix} -1 & -1 \\ -2 & -3 \end{pmatrix} \cdot x \pmod{1}.$$

Referring to the points (1), this map fixes p_0 and p_1 and interchanges p_2 and p_3 . For our purposes, we cut our unit cell for the torus slightly differently, as shown in Fig. 10(a). In addition to p_0 and p_1 , the map has four more fixed points:

$$(8) \quad \left(-\frac{1}{3} \ -\frac{1}{3}\right), \left(\frac{1}{3} \ \frac{1}{3}\right), \left(\frac{1}{6} \ \frac{2}{3}\right), \left(-\frac{1}{6} \ \frac{1}{3}\right).$$

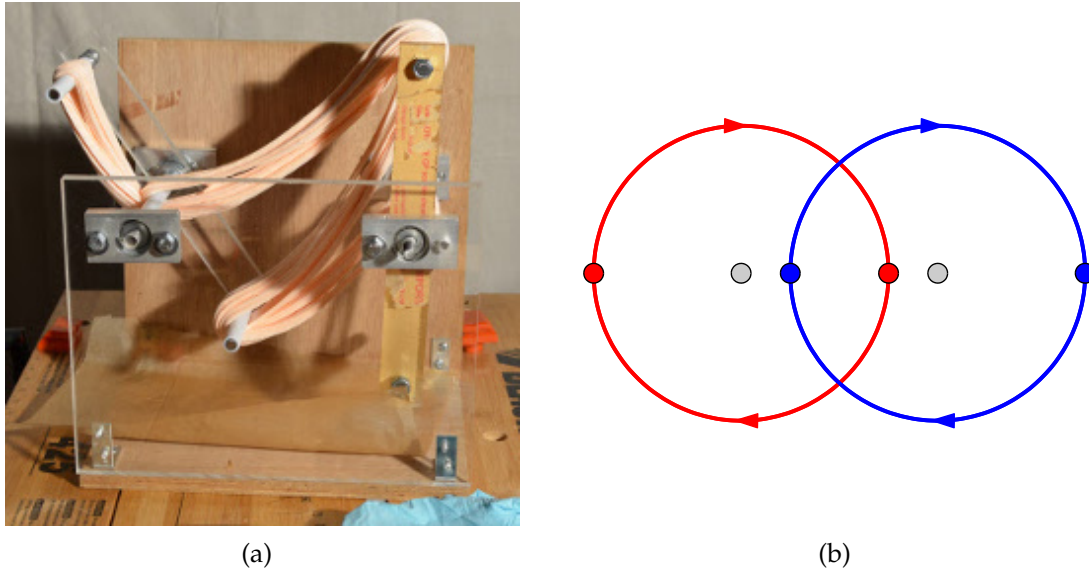


FIGURE 8. (a) A 6-pronged taffy puller designed and built by Alexander Flanagan and the author. (b) The motion of the rods, with two fixed axles.

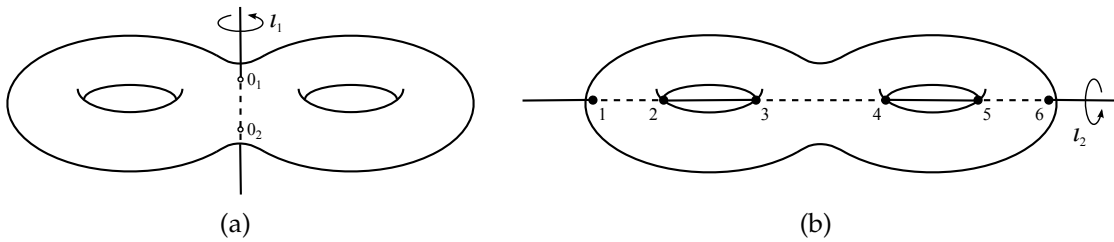


FIGURE 9. The two involutions of a genus two surface S_2 as rotations by π . (a) The involution ι_1 has two fixed points; (b) ι_2 has six.

To create our branched cover of the torus, we will make a cut from the point $0_1 = (-\frac{1}{3} \ -\frac{1}{3})$ to $0_2 = (\frac{1}{3} \ \frac{1}{3})$, as shown in Fig. 10(b). We have also labeled by 1–6 the points that will correspond to our rods. The arrows show identified opposite edges; we have effectively cut a slit in two tori, opened the slits into disks, and glued the tori at those disks to create a genus two surface. The involution ι_1 from Fig. 9(a) corresponds to translating the top half in Fig. 10(b) down to the bottom half; the only fixed points are then 0_1 and 0_2 . For the involution ι_2 of Fig. 9(b), first divide Fig. 10(b) into four sectors with 2–5 at their center; then rotate each sector

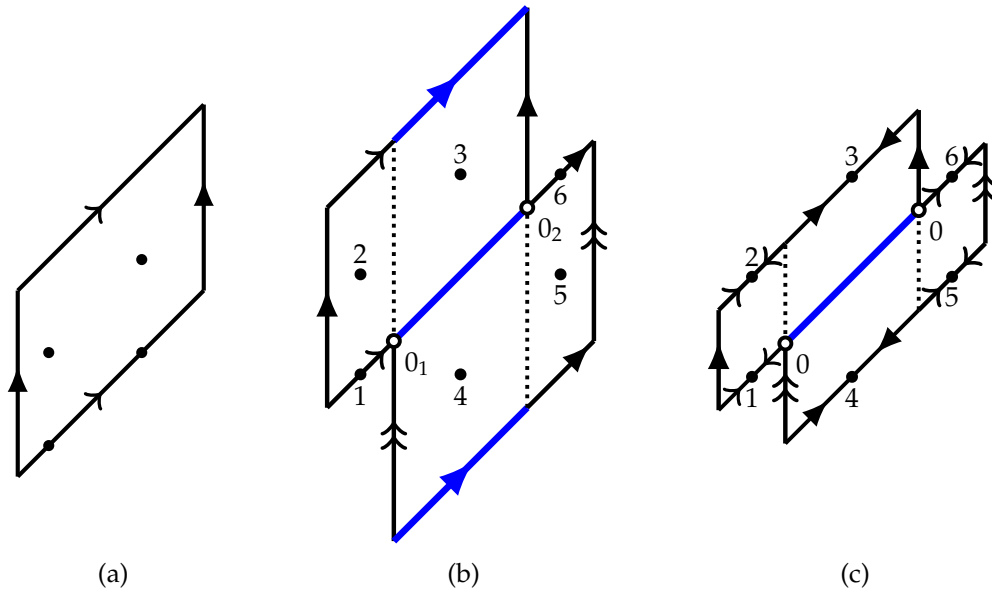


FIGURE 10. (a) A different unfolding of the torus. The four fixed points of ι are indicated. (b) Two copies of the torus glued together after removing a disk. The points $0_{1,2}$ are at $\mp(\frac{1}{3} \frac{1}{3})$. This gives the genus two surface S_2 . The two tori are mapped to each other by the involution ι_1 from Fig 9, with fixed points $0_{1,2}$. The involution ι_2 acts on the individual tori with fixed points $1, \dots, 6$. (c) The quotient surface S_2/ι_2 , which is the punctured sphere $S_{0,6}$.

by π about its center. This fixes the points 1–6. The quotient surface S_2/ι_2 gives the punctured sphere $S_{0,6}$, shown in Fig. 10(c). The points $0_{1,2}$ are mapped to each other by ι_2 and so become identified with the same point 0.

In Fig. 11(a) we reproduce the genus two surface, omitting the edge identifications for clarity, and draw some arcs between our rods. Now act on the surface (embedded in the plane) with the map (7). The polygon gets stretched, and we cut and glue pieces following the edge identifications to bring it back into its initial domain, as in Fig. 11(b). Punctures 2 and 5 are fixed, 1 and 4 are swapped, as are 3 and 6. This is exactly the same as for a half-period of the puller in Fig. 8(b).

After acting with the map we form the quotient surface $S_2/\iota_2 = S_{0,6}$, as in Fig. 11(c). Now we can carefully trace out the path of each arc, and keep track of which side of the arcs the punctures lie. The paths in Fig. 11(c) are identical to the arcs in Fig. 12, and we conclude that the map (7) is the correct description of the six-rod puller. Its dilatation is thus the largest root of $x^2 - 4x + 1$, which is $2 + \sqrt{3}$.

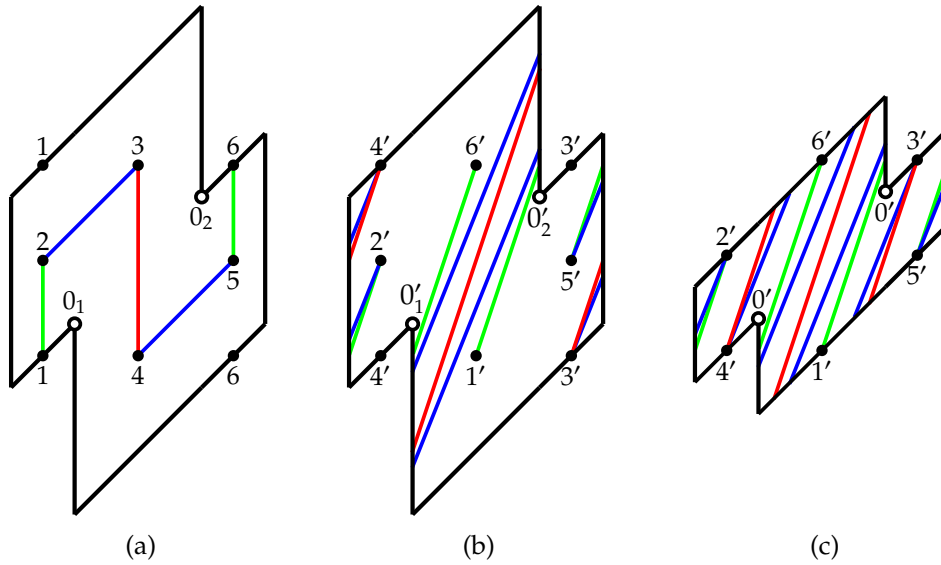


FIGURE 11. (a) The genus two surface from Fig. 10(b), with opposite edges identified and arcs between the rods. (b) The surface and arcs after applying the map (7) and using the edge identifications to cut up and rearrange the surface to the same initial domain. (c) The arcs on the punctured sphere $S_{0,6} = S_2/t_2$, with edges identified as in Fig. 10(c).

The description of the surface as a polygon in the plane, with edge identifications via translations and rotations, comes from the theory of *flat surfaces* (Zorich 2006). In this viewpoint the surface is given a flat metric, and the corners of the polygon correspond to *conical singularities* with infinite curvature. Here, the two singularities $0_{1,2}$ have cone angle 4π , as can be seen by drawing a small circle around the points and following the edge identifications. The sum of the two singularities is 8π , which equals $2\pi(4g - 4)$ by the Gauss–Bonnet formula, with $g = 2$ the genus.

WHAT IS THE BEST TAFFY PULLER?

There are many other taffy puller designs found in the patent literature. (See the Appendix for some examples.) A few of these have a quadratic dilatation, like the examples we discussed, but many don't: they involve pseudo-Anosov maps that are more complicated than simple branched covers of the torus. We will not give a detailed construction of the maps, but rather report the polynomial whose largest root is the dilatation and offer some comments. The polynomials were obtained

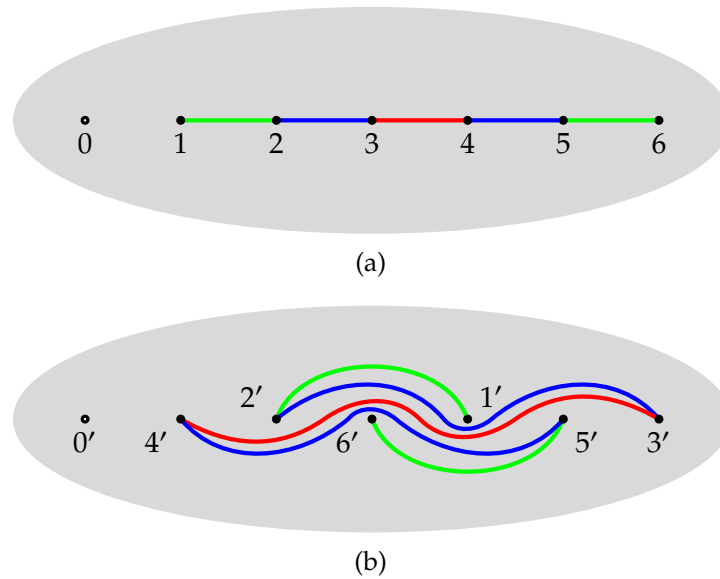


FIGURE 12. (a) A sphere with six punctures (rods) and a seventh puncture at the fixed point 0, with arcs between the punctures, as in Fig. 11(a). (b) The arcs after a half-period of the rod motion in Fig. 8(b). These are identical to the arcs of Fig 11(c).

using the computer programs *braidlab* (Thiffeault and Budišić 2013–2017) and *train* (Hall 2012).

Many taffy pullers are planetary devices — these have rods that move on epicycles, giving their orbits a ‘spirograph’ appearance. The name comes from Ptolemaic models of the solar system, where planetary motions were apparently well-reproduced using systems of gears. Planetary designs are used in many mixing devices, and are a natural way of creating taffy pullers. Kobayashi and Umeda (2007, 2010) and Finn and Thiffeault (2011) have designed and studied a class of such devices.

A typical planetary device, the mixograph, is shown in Fig. 13. The mixograph consists of a small cylindrical vessel with three fixed vertical rods. A lid is lowered onto the base. The lid has two gears each with a pair of rods, and is itself rotating, resulting in a net complex motion as in Fig. 13(c) (top). The mixograph is used to measure properties of bread dough: a piece of dough is placed in the device, and the torque on the rods is recorded on graph paper, in a similar manner to a seismograph. An expert on bread dough can then deduce dough-mixing characteristics from the graph (Connelly and Valenti-Jordan 2008).

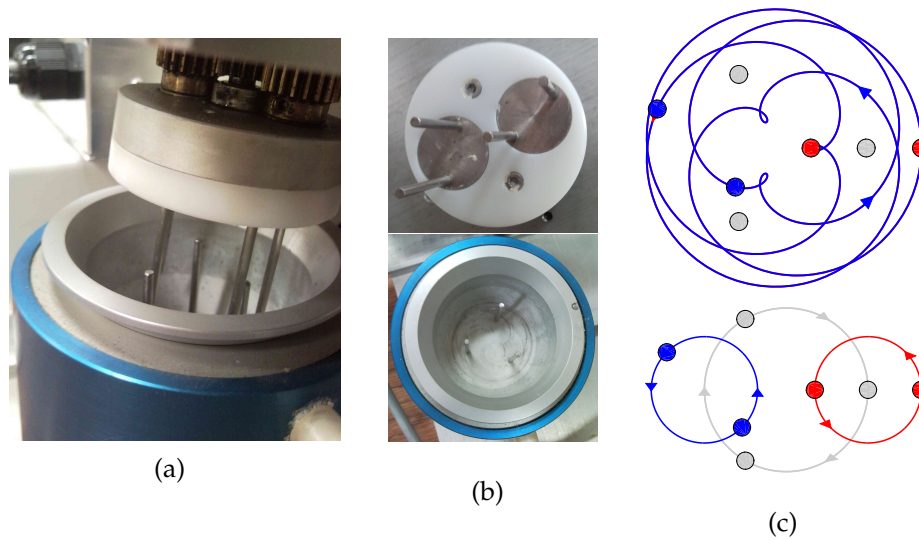


FIGURE 13. (a) The mixograph, a planetary rod mixer for bread dough. (b) Top section with four moving rods (above), and bottom section with three fixed rods (below). (c) The rod motion is complex (top), but is less so in a rotating frame (bottom). (Courtesy of the Department of Food Science, University of Wisconsin. Photo by the author, from Finn and Thiffeault (2011).)

Clearly, passing to a uniformly-rotating frame does not modify the dilatation. For the mixograph, a co-rotating frame where the fixed rods rotate simplifies the orbits somewhat (Fig. 13(c), bottom). The rod motion of Fig. 13(c) (bottom) must be repeated *six* times for all the rods to return to their initial position. The dilatation for the co-rotating map is the largest root of $x^8 - 4x^7 - x^6 + 4x^4 - x^2 - 4x + 1$, which is approximately 4.1858.

The reader might be wondering at this point: which is the best taffy puller? Did all these incremental changes and new designs in the patent literature lead to measurable progress in the effectiveness of taffy pullers? Table 1 collects the characteristic polynomials and the dilatations (the largest root) for all the taffy pullers discussed here and a few others included at the end. The total number of rods is listed (the number in parentheses is the number of fixed rods).

The column labeled p requires a bit of explanation. Comparing the different taffy pullers is not straightforward. To keep things simple, we take the efficiency to be the total dilatation for a full period, defined by all the rods returning to their initial position. For example, referring to Table 1, for the Nitz 1918 device

TABLE 1. Efficiency of taffy pullers. A number of rods such as 6 (2) indicates 6 total rods, with 2 fixed. The largest root of the polynomial is the dilatation. The dilatation corresponds to a fraction p of a full period, when each rod returns to its initial position. The entropy per period is $\log(\text{dilatation})/\text{period}$, which is a crude measure of efficiency. Here $\varphi = \frac{1}{2}(1 + \sqrt{5})$ is the Golden Ratio, and $\chi = 1 + \sqrt{2}$ is the Silver Ratio.

puller	fig.	rods	polynomial	dilatation	p	entropy/ period
standard 3-rod	2	3 (1)	$x^2 - 6x + 1$	χ^2	1	1.7627
Nitz (1918)	3	3	$x^2 - 3x + 1$	φ^2	1/3	2.8873
standard 4-rod	6	4	$x^2 - 6x + 1$	χ^2	1	1.7627
Thibodeau (1904)	14	4	$x^2 - 3x + 1$	φ^2	1/3	2.8873
6-rod	8	6 (2)	$x^2 - 4x + 1$	$2 + \sqrt{3}$	1/2	2.6339
McCarthy (1916) †	15(c)	4 (3)	$x^2 - 18x + 1$	φ^6	1	2.8873
	15(d)	4 (3)	$x^4 - 36x^3 + 54x^2 - 36x + 1$	34.4634	1	3.5399
mixograph ‡	13(c)	7	$x^8 - 4x^7 - x^6 + 4x^4 - x^2 - 4x + 1$	4.1858	1/6	8.5902
Jenner (1905)	16	5 (3)	$x^4 - 8x^3 - 2x^2 - 8x + 1$	$(\varphi + \sqrt{\varphi})^2$	1	2.1226
Shean (1914)	17	6	$x^2 - 4x + 1$	$2 + \sqrt{3}$	1/2	2.6339
McCarthy (1915)	18	5 (2)	$x^4 - 20x^3 - 26x^2 - 20x + 1$	21.2667	1	3.0571

† The McCarthy (1916) device has two configurations.

‡ This is the co-rotating version of the mixograph (Fig. 13(c), bottom).

the rods return to the same configuration (as a set) after $p = 1/3$ period. Hence, the dilatation listed, φ^2 , is for 1/3 period. We define a puller's efficiency as the entropy (logarithm of the dilatation) per period. In this case the efficiency is $\log(\varphi^2)/(1/3) = 6 \log \varphi \approx 2.8873$. By this measure, the mixograph is the clear winner, with a staggering efficiency of 8.5902. Of course, it also has the most rods. The large efficiency is mostly due to how long the rods take to return to their initial position.

Some general observations can be made regarding practical taffy pullers. With a few exceptions, they all give pseudo-Anosov maps. Though we did not define this term precisely, in this context it implies that any initial piece of taffy caught on the rods will grow exponentially. The inventors were thus aware, at least intuitively, that there should be no unnecessary rods. Another observation is that most of the dilatations are quadratic numbers. There are probably a few reasons for this. One is that the polynomial giving the dilatation expresses a recurrence relation

that characterizes how the taffy's folds are combined at each period. With a small number of rods, there is a limit to the degree of this recurrence ($2n - 4$ for n rods). A second reason is that more rods does not necessarily mean larger dilatation (Finn and Thiffeault 2011). On the contrary, more rods allows for a smaller dilatation, as observed when finding the smallest value of the dilatation (Hironaka and Kin 2006; Lanneau and Thiffeault 2011; Thiffeault and Finn 2006; Venzke 2008).

The collection of taffy pullers presented here can be thought of as a battery of examples to illustrate various types of pseudo-Anosov maps. Even though they did not come out of the mathematical literature, they predate by many decades the examples that were later constructed by mathematicians (Binder 2010; Binder and Cox 2008; Boyland, Aref, and Stremler 2000; Boyland and Harrington 2011; Finn and Thiffeault 2011; Kobayashi and Umeda 2007, 2010; Thiffeault and Finn 2006).

Acknowledgments. The author thanks Alex Flanagan for helping to design and build the 6-rod taffy puller, and Phil Boyland and Eiko Kin for their comments on the manuscript.

REFERENCES

- Binder, B. J. (2010). "Ghost rods adopting the role of withdrawn baffles in batch mixer designs." *Phys. Lett. A* **374**, 3483–3486.
- Binder, B. J. and S. M. Cox (2008). "A mixer design for the pigtail braid." *Fluid Dyn. Res.* **40**, 34–44.
- Boyland, P. L., H. Aref, and M. A. Stremler (2000). "Topological fluid mechanics of stirring." *J. Fluid Mech.* **403**, 277–304.
- Boyland, P. L. and J. Harrington (2011). "The entropy efficiency of point-push mapping classes on the punctured disk." *Algeb. Geom. Topology* **11**(4), 2265–2296.
- Connelly, R. K. and J. Valenti-Jordan (2008). "Mixing analysis of a Newtonian fluid in a 3D planetary pin mixer." **86**(12), 1434–1440.
- Dickinson, H. M. (1906). "Candy-pulling machine." Pat. US831501 A.
- Farb, B. and D. Margalit (2011). *A Primer on Mapping Class Groups*. Princeton, NJ: Princeton University Press.
- Fathi, A., F. Laudenbach, and V. Poénaru (1979). "Travaux de Thurston sur les surfaces." *Astérisque* **66-67**, 1–284.
- Finn, M. D. and J.-L. Thiffeault (2011). "Topological optimization of rod-stirring devices." *SIAM Rev.* **53**(4), 723–743.
- Firchau, P. J. G. (1893). "Machine for working candy." Pat. US511011 A.
- Franks, J. and E. Rykken (1999). "Pseudo-Anosov homeomorphisms with quadratic expansion." *Proc. Amer. Math. Soc.* **127**, 2183–2192.

- Halbert, J. T. and J. A. Yorke (2014). "Modeling a chaotic machine's dynamics as a linear map on a "square sphere"." *Topology Proceedings* **44**, 257–284.
- Hall, T. (2012). *Train: A C++ program for computing train tracks of surface homeomorphisms*. http://www.liv.ac.uk/~tobyhall/T_Hall.html.
- Hironaka, E. and E. Kin (2006). "A family of pseudo-Anosov braids with small dilatation." *Algebraic & Geometric Topology* **6**, 699–738.
- Hudson, W. T. (1904). "Candy-working machine." Pat. US752226 A.
- Jenner, E. J. (1905). "Candy-pulling machine." Pat. US804726 A.
- Kirsch, E. (1928). "Candy-pulling machine." Pat. US1656005 A.
- Kobayashi, T. and S. Umeda (2007). "Realizing pseudo-Anosov egg beaters with simple mechanisms." In: *Proceedings of the International Workshop on Knot Theory for Scientific Objects, Osaka, Japan*. Osaka, Japan: Osaka Municipal Universities Press, pp. 97–109.
- (2010). "A design for pseudo-Anosov braids using hypotrochoid curves." *Topology Appl.* **157**, 280–289.
- Lanneau, E. and J.-L. Thiffeault (2011). "On the minimum dilatation of braids on the punctured disc." *Geometriae Dedicata* **152**(1), 165–182.
- MacKay, R. S. (2001). "Complicated dynamics from simple topological hypotheses." *Phil. Trans. R. Soc. Lond. A* **359**, 1479–1496.
- McCarthy, E. F. (1916). "Candy-pulling machine." Pat. US1182394 A.
- McCarthy, E. F. and E. W. Wilson (1915). "Candy-pulling machine." Pat. US1139786 A.
- Nitz, C. G. W. (1918). "Candy-puller." Pat. US1278197 A.
- Richards, F. H. (1905). "Process of making candy." Pat. US790920 A.
- Robinson, E. M. and J. H. Deiter (1908). "Candy-pulling machine." Pat. US881442 A.
- Russell, R. G. and R. B. Wiley (1951). "Apparatus for mixing viscous liquids." Pat. US2577920 A.
- Shean, G. C. C. and L. Schmelz (1914). "Candy-pulling machine." Pat. US1112569 A.
- Thibodeau, C. (1903). "Method of pulling candy." Pat. US736313 A.
- (1904). "Candy-pulling machine." Pat. US772442 A.
- Thiffeault, J.-L. and M. D. Finn (2006). "Topology, braids, and mixing in fluids." *Phil. Trans. R. Soc. Lond. A* **364**, 3251–3266.
- Thiffeault, J.-L. and M. Budišić (2013–2017). *Braidlab: A Software Package for Braids and Loops*. <http://arXiv.org/abs/1410.0849>, Version 3.2.2.
- Thurston, W. P. (1988). "On the geometry and dynamics of diffeomorphisms of surfaces." *Bull. Am. Math. Soc.* **19**, 417–431.
- Tumasz, S. E. and J.-L. Thiffeault (2013a). "Estimating Topological Entropy from the Motion of Stirring Rods." *Procedia IUTAM* **7**, 117–126.
- (2013b). "Topological entropy and secondary folding." *J. Nonlinear Sci.* **13**(3), 511–524.

- Venzke, R. W. (2008). *Braid Forcing, Hyperbolic Geometry, and Pseudo-Anosov Sequences of Low Entropy*. PhD thesis. California Institute of Technology.
- Zorich, A. (2006). "Flat surfaces." In: *Frontiers in Number Theory, Physics, and Geometry*. Ed. by P. Cartier et al. Vol. 1. Berlin: Springer, pp. 439–586.

APPENDIX: A FEW MORE TAFFY PULLER DESIGNS

Because of space constraints, several taffy pullers from the patent literature were omitted from the *Mathematical Intelligencer* version of this article. We include these here for the interested reader.

A 4-rod device with Golden ratio dilatation. Thibodeau's device in Fig. 6 gave an example of a 4-rod taffy puller arising directly from an Anosov map. Another example is a later design of Thibodeau shown in Fig. 14. It consists of three rods moving in a circle, and a fourth rod crossing their path back and forth. This taffy puller can be shown to come from the same Anosov as gave us the 3-rod puller in Fig. 3, with dilatation equal to the square of the Golden Ratio. Thus, if one is interested in building a device with a Golden Ratio dilatation, the design in Fig. 14(a) is probably far easier to implement than Nitz's in Fig. 3(c), since Thibodeau's does not involve rods being exchanged between two gears.

A simple planetary design. McCarthy (1916) has an interesting planetary design for a taffy puller (Fig. 15). It has two configurations, with rod motions shown in Fig. 15(b). Its first configuration (pictured in Fig. 15(a) with rod motion as in Fig. 15(c)) is a perfect example of a ' π_1 -stirring device,' a device where only a single rod moves around a set of fixed rods. The optimality of such devices was studied by Boyland and Harrington (2011), and McCarthy's device is one of their optimal examples.

The second configuration (not shown) involves replacing the chain in Fig. 15(a) by two gears in direct contact. This gives the motion in Fig. 15(d), which does appear quite different from McCarthy's sketch (Fig. 15(b), bottom) but is topologically identical. McCarthy himself seemed to prefer the first configuration, as he noted a bit wordily in his patent:

The planetary course described by this pin, when this modified construction is employed, gives a constant pull to the candy, but does not accomplish as thorough mixing of the same as when said pin describes the planetary course resulting from the construction of the preferred form of my invention, as hereinbefore first described.

What he meant by 'a constant pull to the candy' is probably that in the second configuration the rod moves back and forth in the center of the device, so the taffy would sometimes be unstretched. In the first configuration the rod resolutely

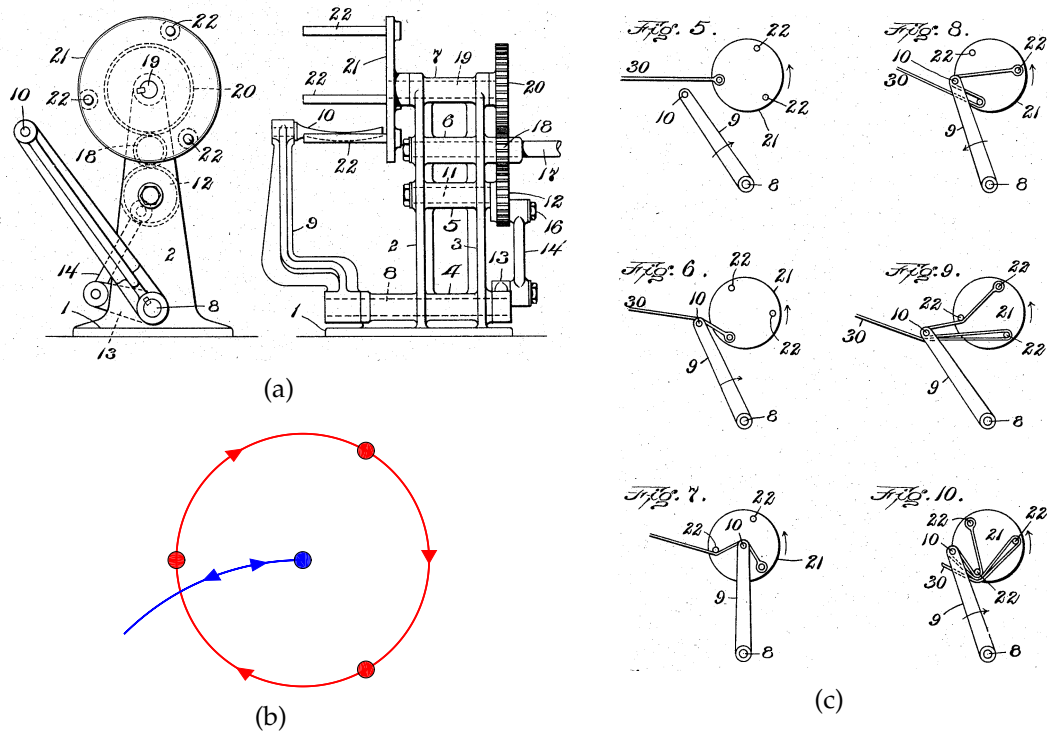


FIGURE 14. (a) Taffy puller from the patent of Thibodeau (1904), with three rotating rods on a wheel and an oscillating arm. (b) Rod motion. (c) The action of the taffy puller, as depicted in the patent.

traverses the center of the device in a single direction each time, leading to uniform stretching. This is related to motions that remain ‘pulled tight’ as the rods move (Tumas and Thiffeault 2013a,b). As far as the less thorough mixing he mentions is concerned, in one turn of the handle the first configuration gives a dilatation of 4.2361, while the second has 2.4229. However, the second design has a larger dilatation for a full period of the rod motion, as given in Table 1. This illustrates the difficulties involved in comparing the efficiency of different devices. In its first configuration the device has a quadratic dilatation, the largest root of $x^2 - 18x + 1$. In its second configuration the dilatation is a quartic number, the largest root of $x^4 - 36x^3 + 5x^2 - 36x + 1$.

A peculiar dilatation. The design of Jenner (1905), shown in Fig. 16, is a fairly straightforward variant of the other devices we’ve seen. From our point of view it has a peculiar property: its dilatation is the largest root of the polynomial $x^4 -$

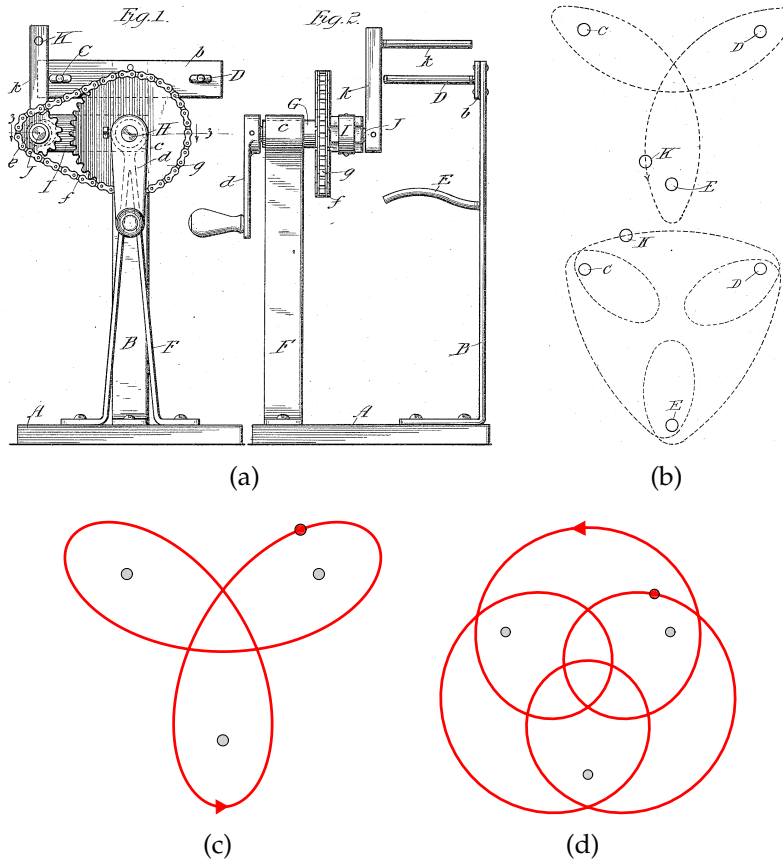


FIGURE 15. (a) Taffy puller from the patent of McCarthy (1916). (b) Rod motion for the two configurations of the device as sketched in the patent. (c) and (d): the actual rod motions.

$8x^3 - 2x^2 - 8x + 1$, which is the strange number $(\varphi + \sqrt{\varphi})^2$, where φ is the Golden Ratio.

Interlocking combs. The taffy puller of Shean and Schmelz (1914) is shown in Fig. 17. The design is somewhat novel, since it is not based directly on gears. It consists of two interlocking ‘combs’ of three rods each, for a total of six moving rods. Mathematically, this device has exactly the same dilatation as the earlier 6-rod design (Fig. 8). A similar comb design was later used in a device for homogenizing molten glass (Russell and Wiley 1951).

A baroque design. We finish with the intriguing design of McCarthy and Wilson (1915), shown in Fig. 18. This is the most baroque design we’ve encountered: it

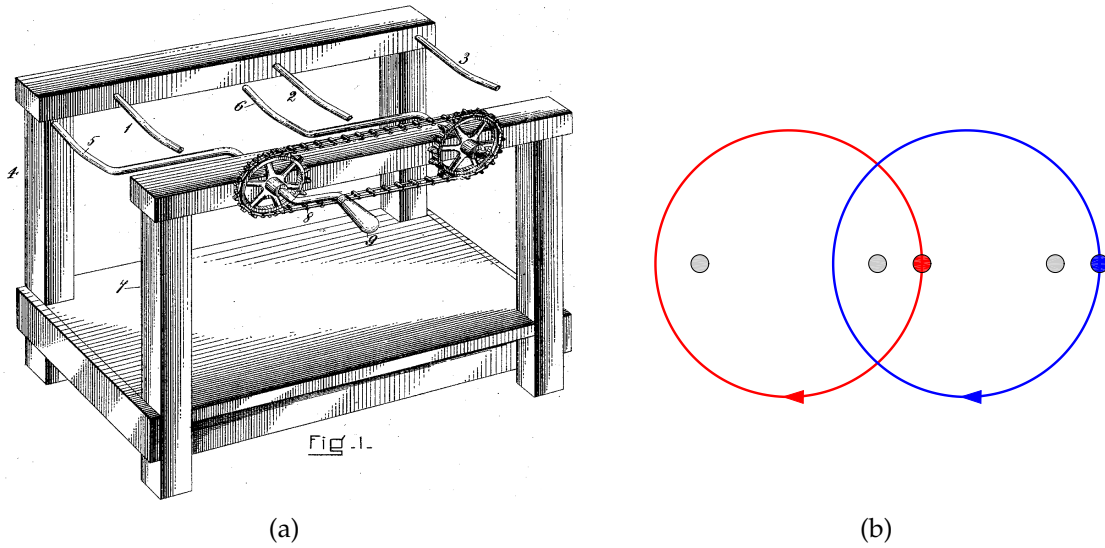


FIGURE 16. Taffy puller from the patent of Jenner (1905). (b) The motion of the rods, with three fixed rods in gray.

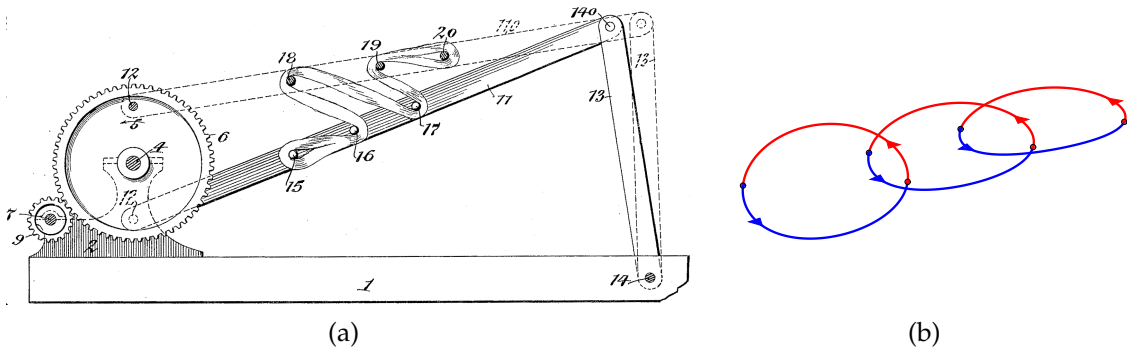


FIGURE 17. (a) Taffy puller from the patent of Shean and Schmelz (1914). (b) The rod motion.

contains an oscillating arm, rotating rods, and fixed rods. The inventors did seem to know what they were doing with this complexity: its dilatation is enormous at approximately 21.2667, the largest root of $x^4 - 20x^3 - 26x^2 - 20x + 1$.

Why so many designs? There are actually quite a few more patents for taffy pullers that were not shown here (only U.S. patents were searched). An obvious question is: why so many? Often the answer is that a new patent is created to

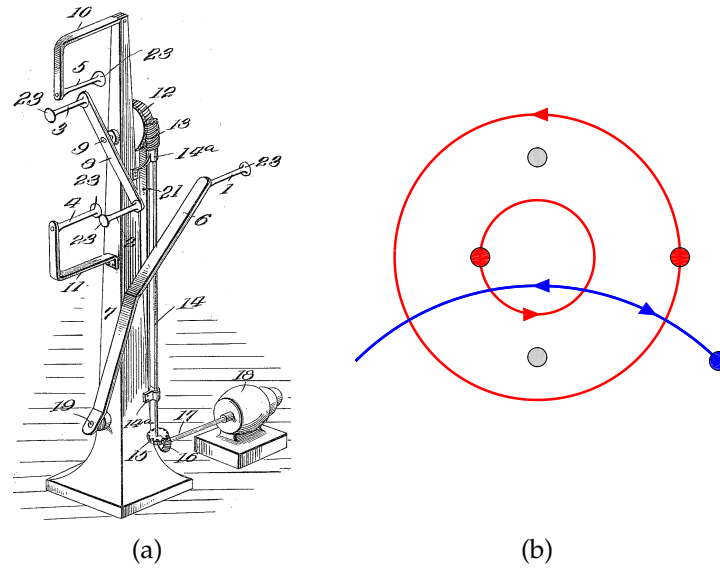


FIGURE 18. (a) Taffy puller from the patent of McCarthy and Wilson (1915). (b) Rod motion.

get around an earlier one, but the very first patents had lapsed by the 1920s and yet more designs were introduced, so this is only a partial answer. Perhaps there is a natural response when looking at a taffy puller to think that we can design a better one, since the basic idea is so simple. At least mathematics provides a way of making sure that we've thoroughly explored all designs, and to gauge the effectiveness of existing ones.

DEPARTMENT OF MATHEMATICS, UNIVERSITY OF WISCONSIN, MADISON, WI 53706, USA
E-mail address: jeanluc@math.wisc.edu